

Benthic Oxygen Consumption and Organic Matter Turnover in Organic-poor, Permeable Shelf Sands

ANTJE RUSCH^{1,3,*}, MARKUS HUETTEL^{1,4}, CHRISTIAN WILD⁵ and CLARE E. REIMERS²

¹Max Planck Institute for Marine Microbiology, Celsiusstr. 1, D-28359 Bremen, Germany;

²Hatfield Marine Science Center, Oregon State University, 2030 South Marine Science Drive,

Newport OR 97365, U.S.A.; ³Present address: Department of Geology and Geophysics, University of Hawaii at Manoa, 1680 East-West Road, Honolulu HI 96822, U.S.A.; ⁴Present address:

Department of Oceanography, Florida State University, Tallahassee FL 32306, U.S.A. ⁵Present address: GeoBio-Center, Ludwig-Maximilians-Universität, Richard-Wagner-Str. 10, 80333 München, Germany

(Received 16 December 2003; accepted 14 January 2005)

Abstract. The high permeability of sediments and strong near-bottom currents cause seawater to infiltrate the surface layers of Middle Atlantic Bight shelf deposits. In this study, sandy sediment cores from 11 to 12 m water depth were percolated with filtered seawater on shipboard. Sedimentary oxygen consumption (SOC) increased non-linearly with pore water flow, approaching maximum rates of 120 mmol m⁻² d⁻¹ (May 2001) or 75 mmol m⁻² d⁻¹ (July 2001). The addition of acetate to the inflowing water promptly enhanced the release of dissolved inorganic carbon (DIC) from the cores. DIC production rates were a linear function of acetate concentration, ranging from 100 to 300 mmol m⁻² d⁻¹ without substrate addition to 572 mmol m⁻² d⁻¹ with 100 mM acetate. The sediments also hydrolyzed a glucose pseudopolymer, and the liberated glucose prompted an increase of SOC. Our results suggest that decomposition rates of organic matter in permeable sands can exceed those of fine-grained, organic-rich deposits, when water currents cause advective interstitial flow, supplying the subsurface microbial community with degradable material and electron acceptors. We conclude that the highly permeable sand beds of the Middle Atlantic Bight are responsive within minutes to hours and efficiently operate as biocatalytical filters.

Key words: benthic mineralization, pore water flow, biocatalytical filter, oxygen, DOM, DIC, permeable sediment, shelf sands

1. Introduction

Organic matter fluxes to the seafloor are often large and highly dynamic in nearshore continental shelf environments (Wollast, 1991). Barely dampened by the shallow water, surface gravity waves and longshore and tidal currents

* Author for correspondence. E-mail: antje@hawaii.edu

tend to redistribute settling organic particulates and carry organic-rich particles across the water/sediment interface and through the near-surface interstices of permeable shelf deposits (Thibodeaux and Boyle, 1987; Forster et al., 1996; Huettel et al., 1996, 1998; Ziebis et al., 1996; Pilditch et al., 1998; Falter and Sansone, 2000; Rusch and Huettel, 2000; Precht et al., 2003; Reimers et al., 2004). Deeper-reaching solute exchange may further enlarge the sediment volume that efficiently participates in organic matter decomposition, and increase turnover rates, so that shelf sands maintain their non-accumulating, organic-poor character (Huettel and Rusch, 2000).

The awareness of dealing with sediment systems that are naturally open and dynamic has led to open-top core incubations (Kristensen and Hansen, 1995; Holmer, 1996; Thomsen and Kristensen, 1997), studies in recirculating flumes (Forster et al., 1996), stirred chamber incubations (Huettel and Rusch, 2000), new interpretations of in situ profiles (Rusch et al., 2000, 2001), and in situ eddy-correlation (Berg et al., 2003) as means to estimate benthic respiration rates.

With the working hypothesis, that flow through permeable sediments enhances the benthic mineralization of organic matter, we investigated the ability of sandy shelf surface sediments to consume oxygen, generate CO₂, and degrade additions of dissolved organic matter (DOM), using flow-through sediment column systems to monitor the influence of interstitial flow. Four sets of experiments were run to quantify

1. the relation between pore water flow rate and degradation rate
2. the metabolic response of the sedimentary microbial community to DOM input in terms of time scales and degradation capacity
3. the relation between the amount of DOM added and degradation rate
4. the rate of extracellular hydrolysis of biopolymers in the sediment

The results are expected to improve our understanding of the coupling between hydrodynamical conditions and the capture and decomposition of organic matter in shelf sands, and their potential role in the cycling of organic matter in shelf environments.

2. Materials and Methods

2.1. STUDY SITE AND SAMPLING

The experimental study was carried out with sediment cores retrieved from the sandy shelf of the Middle Atlantic Bight offshore of Tuckerton, New Jersey, U.S.A. The sampling site (39°27' N, 074°14' W) was located within a region that contains the Long-term Ecosystem Observatory at ca. 15 m water depth (LEO-15; map e.g., in, Scala and Kerkhof, 2000). Relatively strong wind- and wave-induced currents frequently reach the bottom of these

shallow waters, so that near-bottom velocities are generally 0.10 m s^{-1} or even greater (Styles, 1998). Episodic upwelling of offshore bottom waters into surface layers can last for days or weeks and lead to high abundances of phytoplankton (Kerkhof et al., 1999), such as observed during the May 01 and July 01 cruises (Rusch et al., 2003).

On 08 December 00, 30 May 01 and 24 July 01, sediment cores (3.6 cm i.d., 6–10 cm long) were retrieved by scuba-divers for the shipboard flow-through experiments. These well-sorted medium to coarse sands (median grain size 400–500 μm) had a porosity of 0.37, and permeabilities were in the order of 10^{-11} m^2 (Reimers et al., 2004). The organic carbon content ranged between 0.015% and 0.030% (Rusch et al., 2003).

2.2. EXPERIMENTAL SETUP

Immediately after retrieval, the cores were mounted to a stand and transferred into a water tank held at constant (within $\pm 0.2 \text{ }^\circ\text{C}$) temperature close to that of the bottom water, i.e., $6 \text{ }^\circ\text{C}$ in December 00, $13 \text{ }^\circ\text{C}$ in May/June 01, and $21 \text{ }^\circ\text{C}$ in July 01. The pierced rubber stoppers on both ends of each core (Figure 1) were connected to 1.02-mm Tygon™ tubing. The overlying water volume in the columns was reduced to less than 5 mL by replacing a major part with pierced styrodur™ disks to minimize oxygen consumption by the overlying water. Light was excluded by wrapping all columns in aluminum foil.

Filtered (0.2 μm) local seawater was pumped from an isothermal reservoir through the cores at different flow rates, and varying amounts of different organic carbon compounds were added to the inflowing water via a three-way stopcock. The concentrations of oxygen and dissolved inorganic carbon (DIC) were measured in the inflowing and outflowing water.

Four sets of experiments aimed to quantify the extent and time scales of sedimentary DOM decomposition in different settings:

1. different pore water flow rates (*Flow rate experiment*)
2. with and without addition of acetate (*Spike experiment*)
3. different acetate concentrations (*Concentration experiment*)
4. addition of 4-methylumbelliferyl- β -D-glucoside (MUF-Glu) as a pseudo-polymeric substrate (*Hydrolysis Experiment*).

In the *Flow Rate Experiment*, conducted on 31 May 01, no substrate was added, and up to 8 cores were exposed to pore water flow at rates of 21–30, 14, 40–44, 53–62, 4–5, 53–62, and again 53–62 mL h^{-1} (in this order). Each core was monitored for at least the time needed for a pore water front to migrate through the full length of the core. Oxygen consumption was calculated as $([\text{O}_2]_{\text{in}} - [\text{O}_2]_{\text{out}})/(A \times \Delta t)$, with A : cross-sectional area of the core; Δt : residence time.

In the *Spike Experiment* (Table I), 50 mL of acetate solution (80 mM in filtered seawater) was pumped through two cores; the pumping rate of



Figure 1. Setup of the columns, not to scale. While particle-free local seawater was pumped through the sediment cores, O₂ concentrations in both the inflowing and the outflowing water were measured by microsensors. The outflowing water was collected in graded glass syringes to determine the flow rate, and to obtain samples for the analysis of reaction products.

50 mL h⁻¹ corresponded to a pore water front migrating at 15.2 cm h⁻¹. Oxygen consumption and DIC production were monitored over time. A similar approach was used in the *Concentration Experiment*, where 16 cores were supplied with different amounts of acetate (Table II) in 50 mL filtered seawater, corresponding to concentrations between 0 and 102 mM.

In the *Hydrolysis Experiment* (Table III), MUF-Glu addition was used to trace the hydrolytic degradation of polysaccharides, generally one of the initial reactions in aerobic and anaerobic decomposition of polymeric DOM. The fluorochromic reaction product methylumbelliferone (MUF) was collected in the outflowing water, 1.5 mL subsamples were preserved by adding 50 μL of 1 N NaOH and stored dark at -20 °C until analysis. MUF concentrations were measured using a Hitachi F-2000 spectrofluorometer to determine the potential activity of extracellular β-glucosidases in the cores (Boetius and Lochte, 1994; Bélanger et al., 1997).

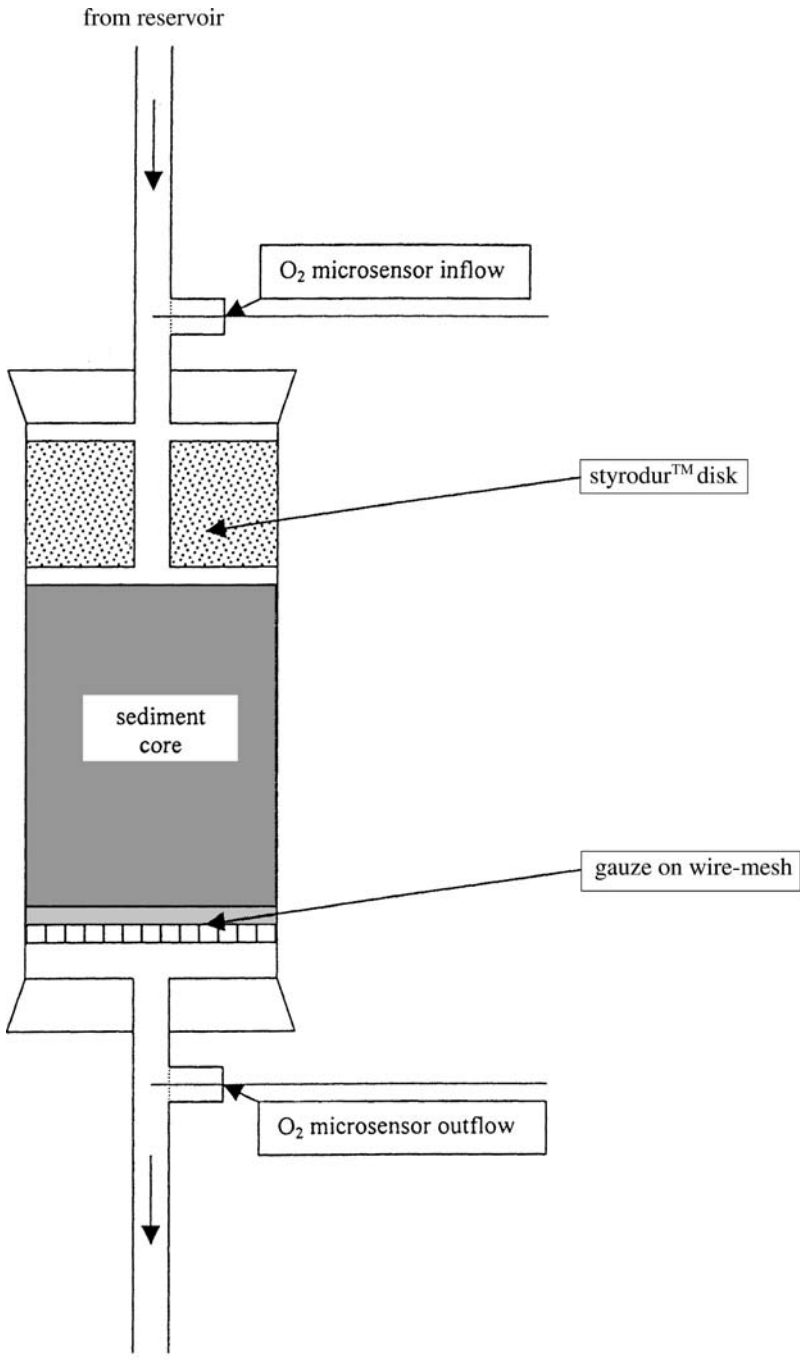
2.3. OXYGEN MEASUREMENTS

To determine oxygen consumption in the sediment cores, flow-through cells with fiber-optic oxygen microsensors (PreSens GmbH, Sensor type B2, tip diameter <50 μm, for the measuring principle, see Klimant et al., 1995) were connected to receive the inflow and outflow of each core (Figure 1). The microsensors were connected to an oxygen meter (Microx-TX, PreSens) with integrated signal processing software. The sensors were calibrated before and after each experiment using a two-point calibration in oxygen-free (addition of sodium dithionite) and air-saturated (bubbled) seawater. Additionally, oxygen concentrations in the reservoir were measured using Winkler titration (Winkler, 1888).

In the December 00 experiments, also Clark type microelectrodes (Revsbech, 1989) were used to measure oxygen concentrations in the inflowing and outflowing water. They were calibrated in the same way as the fiber-optic microsensors, except that yeast instead of dithionite was used to generate oxygen-free water.

2.4. DIC ANALYSES

The outflowing water from each column was collected in 50 mL glass syringes (Figure 1), from which subsamples were taken at regular time intervals and immediately preserved with HgCl₂ for later analysis. DIC



to peristaltic pump and glass syringes

Table 1. The spike experiment, conducted on 09/10 Dec 2000, exposed cores D1–D4 to pore water flow at a rate of 50 mL h⁻¹.

Core	T in °C	Flow history		Oxygen consumption in mmol m ⁻² d ⁻¹		DIC production in mmol m ⁻² d ⁻¹	
		Stagnancy	Flow	Before	After	Before	After
D1	12	12 h	3 h	79.2	94.6	107	141
	7–10	8 h	3 h	36.6		105	
D2	12	12 h	3 h	93.0	85.9	108	139
	7–10	8 h	3 h	64.0		108	
D3	7–9	<1 h	1 h	19.6		106	
D4	7–9	<1 h	1 h	8.9		111	

Temperatures refer to the outflowing water. Flow history – stagnancy: the time between retrieval of the cores and start of the percolation. Flow history – flow: the time between start of the percolation and start of the data collection. The inflowing water of cores D1 and D2 was “spiked” with acetate (4 mmol). The rates of sedimentary oxygen consumption and dissolved inorganic carbon (DIC) production before and after the addition of acetate are given as weighted averages, i.e., integrated over time, then divided by total time.

concentrations were measured using a flow injection system as described by Hall and Aller (1992). Freshly prepared NaHCO₃ solutions were used for calibration. The detection limit was 0.05 mM, and the analytical precision was 0.01 mM.

2.5. MICROBIAL CELL COUNTS

After the experiments, 50 cm³ sediment were preserved by addition of 10 mL filtered seawater containing formalin (final conc. 3.5%) and stored at 4 °C until analysis. To dislodge cells from the sand grains, the samples were subjected to ultrasonic treatment (30% pulsed, Bandelin M72 probe) for 150 s and washed with 8 × 5 mL Na₄P₂O₇ solution (10 mM). Aliquots of the resulting cell suspension were concentrated on polycarbonate membrane filters (0.2 μm pore size) and stained with acridin orange. Epifluorescence microscopy (Zeiss Axioskop) at 1300 × magnification was used to determine cell numbers in 25 randomly chosen fields of view.

3. Results

3.1. UNAMENDED SEDIMENTS

In the water percolating through cores without experimentally added organic compounds, oxygen concentrations decreased to typically 70–85% saturation, and DIC concentrations increased to 2.0–2.5 mM. These changes reflect the decomposition of natural organic matter and respiration by the microbial

Table II. The concentration experiment, conducted on 01 Jun 2001 at $T = 15\text{ }^{\circ}\text{C}$, exposed cores M1–M16 to pore water flow at a rate of 50 mL h^{-1} , with acetate added to the inflowing water at different concentrations.

Core	Acetate addition (mmol)	Oxygen consumption		DIC production				
		Rate in $\text{mmol m}^{-2}\text{ d}^{-1}$		Rate in $\text{mmol m}^{-2}\text{ d}^{-1}$		Maximum reached		
		Before	After	Onset increase	After		Onset increase	
M1–M8	–	72 to 106						
M9	5.12	308	204	214	60 min	572	90 min	165 min
M10	2.56	261	212	238	30 min	507	60 min	120 min
M11	1.28	193	177	184	60 min	304		
M12	0.64	208	144	167	60 min	327	?	?
M13	0.32	239	203	213	30 min	298		
M14	0.16	240	170	180	60 min	290		
M15	0.08	217	185	200	30 min	292		
M16	–	184 / 66						

Cores M1–M8 had experienced 10 h of stagnancy (after being used in our flow rate experiment), and measurements started 2 h after percolation resumed. In M9–M16, percolation started 1 h after retrieval of the cores; italicized results were obtained after 3 h, all others after 1 h of pore water flow. Oxygen consumption rates before and after acetate addition are given as weighted averages, i.e., integrated over time, then divided by total time. Onset increase: the time between acetate addition and the onset of increased oxygen consumption; at the end of the experiment, maximum rates had not been reached yet. Rates of dissolved inorganic carbon (DIC) production before the addition of acetate were excluded from the data set, as the DIC concentration of the inflowing water appeared erroneously high. ?: temporal resolution or duration of the experiment not sufficient.

Table III. The hydrolysis experiment was conducted on 24/25 July 01 at $T = 22\text{ }^{\circ}\text{C}$ with cores J1–J8, that had been used earlier in a flow rate experiment by Reimers et al. (2004).

Core	Flow history		Flow rate mL h^{-1}	Substrate addition μmol	Oxygen consumption		DIC production		
	Stagnancy	Flow			Rate in $\text{mmol m}^{-2} \text{d}^{-1}$	Onset increase	Maximum reached	Rate in $\text{mmol m}^{-2} \text{d}^{-1}$	
			Before	After	Before	After	Before	After	
J1	6 h	8 h	26–28	4.67 glucose	37.9	56.1	35 min	185 min	49.7
J2	6 h	8 h	26–28	4.50 glucose	38.9	65.0	65 min	155 min	102
J3	6 h	16 h	26–28	–	49.8	–	–	–	147
J4	6 h	12 h	23–26	136 MUF-Glu	46.1	62.6	50 min	220 min	56.1
J5	6 h	20 h	12–13	–	56.3	–	–	–	87.3
J6	6 h	21 h	13	–	45.8	–	–	–	–75.0
J7	6 h	16 h	11–12	–	54.9	–	–	–	–27.6
J8	6 h	12 h	12–13	68 MUF-Glu	39.3	57.2	120 min	270 min	75.0

Flow history – stagnancy: the time between the end of the prior experiment and resumed percolation. Flow history – flow: the time between start of the percolation and start of the data collection. MUF-Glu: methylumbelliferyl- β -D-glucose. Glucose and MUF-Glu were supplied at concentrations of 1 and 20 mM, respectively, corresponding to volumes of less than 7 mL. The rates of sedimentary oxygen consumption before and after substrate addition are given as weighted averages. Onset increase: the time between substrate addition and the onset of increased oxygen consumption. Measurements of dissolved inorganic carbon (DIC) concentrations after substrate addition lacked sufficient temporal resolution to allow for the determination of turnover rates. Cores J6 and J7 seemingly removed DIC from the percolating water; these rates should be viewed with caution.

and meiobenthic community; rates are compiled in Table I (December 00), Table II (May/June 01), and Table III (July 01). Macrofauna abundance in these sediments was low: e.g., in July, no more than two individuals per core were found (J1: 1 small bivalve, J2: 1 small shrimp, J3: 1 polychaete, J4: none, J5: 1 amphipod, J6: 2 small polychaetes, J7: 2 small amphipods, J8: none). With oxygen consumption rates of macrofauna typically ranging between 0.45 and 1.34 $\mu\text{mol g}_{(\text{wet})}^{-1} \text{h}^{-1}$ (Newell, 1970), macrofaunal respiration in our cores was estimated at less than 3.15 $\text{mmol m}^{-2} \text{d}^{-1}$.

In December, bacterial abundances in the upper sediment layers ranged from 2 to 4 $\times 10^8 \text{ cm}^{-3}$, without significant differences down to 7 cm depth. Sedimentary oxygen consumption ranged between 9 and 93 $\text{mmol m}^{-2} \text{d}^{-1}$. Differences between the cores reflect not only the patchiness of the sampling site, but also their shipboard history with respect to periods with or without water flow (Table I).

Bacterial abundance and oxygen consumption rates in May/June 2001 exceeded those of December 2000. Microbial cell abundance was $7.9 \pm 3.0 \times 10^8 \text{ cm}^{-3}$, and oxygen consumption rates were 72–106 $\text{mmol m}^{-2} \text{d}^{-1}$ in cores M1–M8, and 144–308 $\text{mmol m}^{-2} \text{d}^{-1}$ in cores M9–M16 before substrate addition (Table II). In July, we observed lower bacterial abundances (1 to 2 $\times 10^8 \text{ cm}^{-3}$) and lower SOC than in May/June (Table III).

The rates of DIC release exceeded oxygen consumption in all cores in December (Table I) and most cores in July (Table III), indicating anaerobic mineralization, carbonate dissolution, and/or the absence of steady state.

3.2. FLOW RATE EXPERIMENT

In situ experiments conducted during the July 2001 cruise documented bottom water moving tracer fronts into the sediment at vertical velocities ranging from 53 cm h^{-1} at 0.4 cm depth to 6 cm h^{-1} at 2.0 cm depth (Reimers et al., 2004), with presumably continued decrease at greater depth. These velocities were measured when surface waves were only 0.2–0.3 m high; under less calm conditions, faster and deeper pore water flow can be expected. With flow rates of 4–62 ml h^{-1} in cores M1–M8 and a sediment porosity of 0.31 ± 0.11 ($n = 3$), the pore water front moved through the cores at velocities ranging from 1.3 to 19.6 cm h^{-1} , thus reflecting realistic conditions. The significant increase of oxygen consumption rates with flow rate (Figure 2) can be described as $\text{SOC} = \text{SOC}_{\text{max}} \times \text{flow rate} / (\text{flow rate} + \text{constant})$. An earlier analysis of measurements associated with cores J1–J8 also showed oxygen consumption to vary with flow rate (Reimers et al., 2004). It should be remarked here, however, that SOC was computed differently in Reimers et al. (2004): Based on the assumption that all parts of the sediment column contribute homogeneously to oxygen consumption, SOC was normalized to a core length of 4 cm, which had been determined as

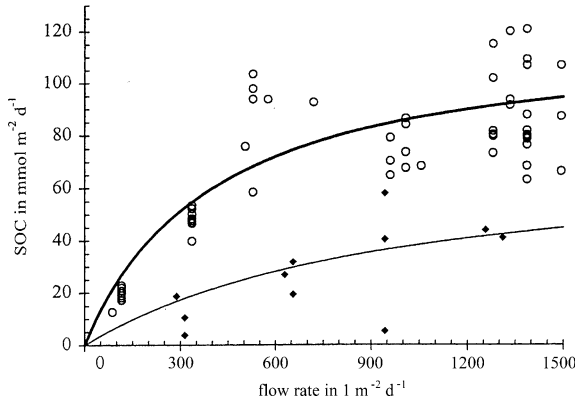


Figure 2. Rates of sedimentary oxygen consumption (SOC) for different flow rates applied to 8 cores in May 01 (circles, bold trendline) and to 6 cores in July 01 (diamonds, fine trendline). The July data represent results of Reimers et al. (2004) after different computation of SOC (for details see text). Trendline equations:

$$\text{SOC (May)} = 120 \text{ mmol m}^{-2} \text{ d}^{-1} \times \text{flow rate} / (\text{flow rate} + 400 \text{ L m}^{-2} \text{ d}^{-1});$$

$$n = 55, \quad r^2 = 0.71.$$

$$\text{SOC (July)} = 75 \text{ mmol m}^{-2} \text{ d}^{-1} \times \text{flow rate} / (\text{flow rate} + 1000 \text{ L m}^{-2} \text{ d}^{-1});$$

$$n = 12, \quad r^2 = 0.70.$$

the *in situ* oxygen penetration depth. This computational approach to correct for differences in core length, however, cannot correct for the experimental uncertainty associated with vertical heterogeneity in respiration rates. To avoid any assumptions about oxygen consumption as a function of sediment depth, and to make results comparable between experiments, all rate estimates, including results from July 2001 given in Reimers et al. (2004), are presented here without normalization. The oxygen consumption rates in July behaved differently depending on whether they were measured early (after <7 h) or late (after >16 h) in the experiment. The late SOC rates in cores J1–J8 ranged between 51 and 76 $\text{mmol m}^{-2} \text{ d}^{-1}$, independent of flow rate (data not shown). The early SOC rates significantly increased with flow rate (Figure 2), following a function of the same type as in the data set from cores M1–M8, which were entirely early measurements. The asymptotic maximum rates were $\text{SOC}_{\text{max}} = 120 \text{ mmol m}^{-2} \text{ d}^{-1}$ in May and $75 \text{ mmol m}^{-2} \text{ d}^{-1}$ in July. The flow rate at which $\text{SOC} = 0.5 \times \text{SOC}_{\text{max}}$ was $400 \text{ L m}^{-2} \text{ d}^{-1}$ in May and $1000 \text{ L m}^{-2} \text{ d}^{-1}$ in July.

3.3. SPIKE EXPERIMENT: ADDITION OF ORGANIC CARBON

The addition of acetate to the inflowing water of cores D1 and D2 (Table I) led to a prompt increase of DIC production, with almost identical time

courses in both cores (Figure 3). DIC production rates started to rise from initially 107 and 108 $\text{mmol m}^{-2} \text{d}^{-1}$ to 155 and 153 $\text{mmol m}^{-2} \text{d}^{-1}$ in D1 and D2, respectively, after 35 min of water passage through the cores (Figure 3). The maximum rates were reached after 75 min and remained at a similar level during the rest of the experiment (total 3.5 h).

The increase of DIC production rates was accompanied by an increase of oxygen consumption rates after 45 min, which was faster and more pronounced in D1 than in D2 (Figure 3). With respect to maximum rates, the cores differed by 33% in oxygen consumption as compared to 1.6% in DIC production. The weighted averages (integrated over time, then divided by total time) of oxygen and DIC turnover rates are summarized in Table I.

3.4. CONCENTRATION EXPERIMENT

The weighted averages of oxygen and DIC turnover rates are summarized in Table II. In both the spike experiment and the concentration experiment, the time-integrated turnover was higher in terms of carbon than in terms of oxygen; DIC production exceeded SOC by a factor of 1.4 to 2.7.

SOC and DIC release depended on the amount of organic carbon supplied (Figure 4). The rate of DIC release was significantly correlated to the amount of acetate added to the cores ($r = 0.96$, $n = 7$, $\alpha < 1\%$). Apparently, oxygen consumption was slightly increased by the addition of acetate (Figure 4), however, not correlated to acetate concentration. The fraction of acetate carbon that was turned over to DIC within 3.25 h after addition ranged from less than 1% in M9 to 30% in M15.

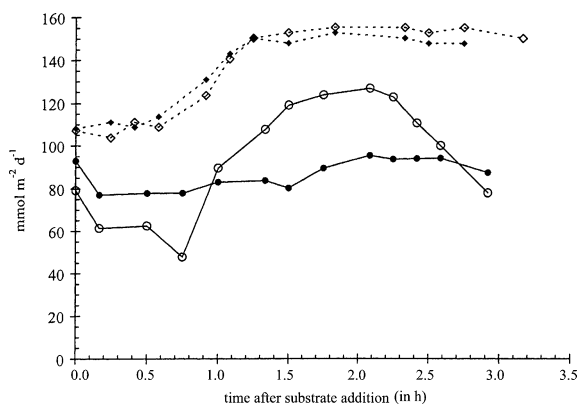


Figure 3. In the spike experiment, conducted in December 2000 at a flow rate of 50 mL h^{-1} , the inflowing water of cores D1 and D2 was “spiked” with acetate (4 mmol). Rates of sedimentary oxygen consumption (circles) and release of dissolved inorganic carbon (diamonds) were monitored over time. Open symbols: core D1; closed symbols: core D2. Values at time 0 are averages over the steady phase preceding acetate addition.

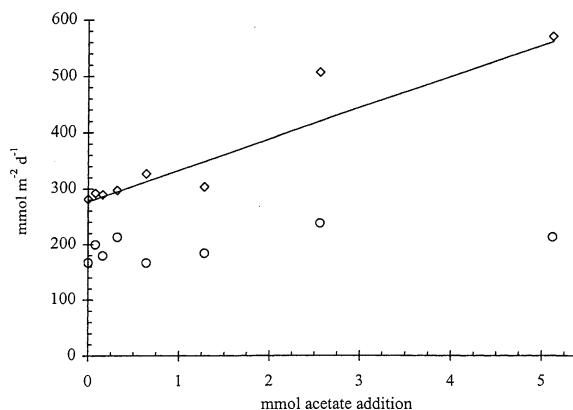


Figure 4. The concentration experiment of 01 June 01 exposed 8 cores to pore water flow at a rate of 50 mL h⁻¹. Different amounts of acetate added to the inflowing water had no significant effect on the time-integrated rates of sedimentary oxygen consumption (circles). The time-integrated rates at which dissolved inorganic carbon (DIC) was released from the cores (diamonds), however, showed a linear correlation with the amount of acetate added: DIC release rate = 277 mmol m⁻² d⁻¹ + 55.8 m⁻² d⁻¹ × acetate addition ($n = 7$, $r^2 = 0.96$, core M10 excluded).

3.5. HYDROLYSIS EXPERIMENT

Similar to the results we obtained with acetate, the addition of pseudo-polymeric MUF-Glu to cores J4 and J8 (Table III) caused an immediate reaction in the sediment, raising oxygen consumption rates while the substrate was hydrolyzed (Figure 5). As an estimate of the hydrolysis of β -glucosides [MUF] in the outflowing water was integrated over time. Core J4 and J8 released 42.2 and 79.7 μmol of MUF, respectively. These values, compared to the amount of MUF-Glu added to the cores, imply complete hydrolysis in core J8, whereas only 31% of the substrate was hydrolyzed in J4, where faster flow (Table III) may have limited the absorption of substrate. While [MUF] decreased steeply after reaching the maximum, SOC remained elevated and decreased more slowly, without returning to the initial rates by end of the experiment (Figure 5).

4. Discussion

A fundamental difference between fine-grained, cohesive sediments and coarse-grained, permeable sediments is the mode of transport of particulate and dissolved material through the upper layers of the bed (Thibodeaux and Boyle, 1987; Huettel and Gust, 1992). In permeable sediments, interstitial transport is dominated by advective pore water flow, which is not only faster than diffusive transport, but also characterized by velocities that are heterogeneous in both space and time (Webb and Theodor, 1968; Huettel and

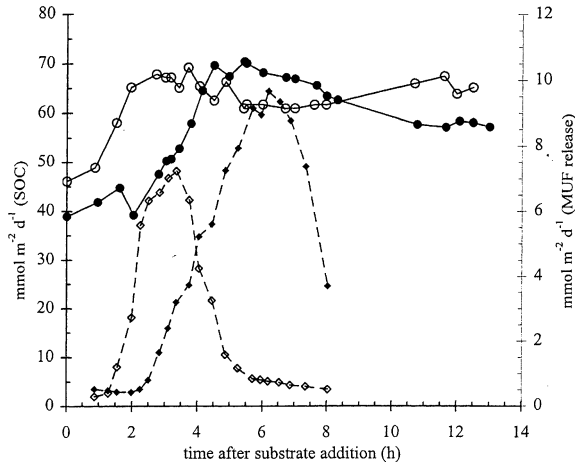


Figure 5. In the hydrolysis experiment, a pulse of methylumbelliferyl- β -D-glucose (20 mM) was supplied to cores J4 (open symbols) and J8 (closed symbols) at a flow rate of 23–26 mL h⁻¹ and 12–13 mL h⁻¹, respectively. The rates of sedimentary oxygen consumption (SOC, circles) and release of the hydrolysis product methylumbelliferone (MUF, diamonds) were recorded over time. Values at time 0 are averages over the steady phase preceding substrate addition.

Gust, 1992). In cohesive sediments, by contrast, solute transport is dominated by diffusion, which is important also in permeable sediments, below the advectively flushed layer. Optode measurements by Precht et al. (2003) showed that the diffusive gradient at the lower boundary of the flushed horizon in permeable sediments can be as steep as at the sediment-water interface of fine-grained deposits.

The vast majority of bacteria living in marine sediments are attached to sediment grains (e.g., Rusch et al., 2001, 2003). Thus, bacterial communities in fine-grained beds depend on either motility or diffusive transport of solutes. In permeable beds, by contrast, relatively fast advective pore water flows provide sessile (micro)organisms with substrates and efficient removal of degradation products (Huettel et al., 1998). Our experiments show that the benthic microbial community of coarse-grained permeable sands of the Middle Atlantic Bight (MAB) shelf can react promptly to the inflow of dissolved organic matter, which is degraded at rates that depend on the velocity of pore water flow.

The *spike experiment* demonstrated this prompt response to the advective inflow of acetate (Figure 3), and similar behavior was observed after the addition of MUF-Glu in the hydrolysis experiment (Figure 5). The time course and extent of these reactions varied between cores and between oxygen and DIC, as to be expected from sandy sediments, considering their naturally complex pattern of spatiotemporal heterogeneity. The response of

the benthic microbial population to the supply of acetate and oxygen may differ considerably, depending on the frequency and duration of previous exposure to organic carbon and electron acceptors of varied quality and quantity, that can stimulate or compete with the utilization of experimentally added substrates. Generally, the microbial community of permeable sands should be well adapted to transient state situations and the need for quick responses. In fine-grained, diffusion dominated sediments, only the microbial film growing on the sediment surface can react to changes in the water column, while subsurface bacteria depend on the comparatively slow diffusive transport of metabolic substrates.

Bacterial cell abundances of 1 to $8 \times 10^8 \text{ cm}^{-3}$ in the MAB sands were an order of magnitude lower than those reported for fine-grained coastal deposits (e.g., Llobet-Brossa et al., 1998; Böttcher et al., 2000; Wilde and Plante, 2002). However, the volume specific surface area of silt exceeds that of sand by a factor of about 4–11 (Skopp, 2000), suggesting similar cell density per grain surface area. *In situ* measurements at our site showed advective flushing down to 4 cm below the sediment surface (Reimers et al., 2004) as compared to 1–3 mm in fine-grained shelf deposits (Andersen and Helder, 1987; Böttcher et al., 2000), so that the total grain surface area exposed to flowing water within a m^2 of sandy sea floor can be up to 10-fold of that of a silty site. Accordingly, several times more bacteria are exposed to the bottom water in permeable sands compared to cohesive sediments, suggesting a higher efficiency in decomposing bottom water solutes and more intense benthic-pelagic coupling.

The degradation capacity of MAB sands was tested in the *concentration experiment*, measuring DIC production rates of 290–572 $\text{mmol m}^{-2} \text{ d}^{-1}$ (Table II), depending on the amount of acetate added to the cores. In unamended sediment, DIC was released at rates of up to 147 $\text{mmol m}^{-2} \text{ d}^{-1}$, which corresponds to 20 $\mu\text{mol cm}^{-3} \text{ d}^{-1}$. Sandy sediments from Danish shallow water sites, studied by open-top core incubations, showed rates of 18–40 $\text{mmol m}^{-2} \text{ d}^{-1}$ (Kristensen and Hansen, 1995), 126–150 $\text{mmol m}^{-2} \text{ d}^{-1}$ (Holmer, 1996), and 4.9–5.6 $\mu\text{mol cm}^{-3} \text{ d}^{-1}$ (Thomsen and Kristensen, 1997), and DIC depth profiles in an intertidal sandflat suggested rates between 1.7 and 48 $\text{mmol m}^{-2} \text{ d}^{-1}$ (Rusch et al., 2000). Although these sands may differ from the MAB sediments with respect to availability of labile organic matter, the higher rates in our experiment may also be linked to the interstitial flow applied.

In fine-grained sediments, the small reach and velocity of diffusive transport limit the amount of oxygen that can be carried into the bed to less than 100 $\text{mmol m}^{-2} \text{ d}^{-1}$ (Røy et al., 2002). Advective pore water transport in permeable sands can enhance oxygen consumption to rates of up to 300 $\text{mmol m}^{-2} \text{ d}^{-1}$ (Table II), as measured at realistic flow velocities in our experiments. Assuming that using oxygen as the final electron acceptor is the

most efficient metabolic pathway for organic matter degradation (Dauwe et al., 2001), these results imply that sand beds more efficiently degrade dissolved organic matter than their fine-grained counterparts. The efficiency of solute decomposition in the MAB sediments may be deduced from the concentration experiment, which showed that 1–30% of the added acetate carbon was turned over to DIC within 3.25 h, corresponding to an average rate of 0.23–0.50 mM h⁻¹. The finding that DIC production exceeded oxygen consumption in the acetate amended cores indicates that part of the organic carbon may be oxidized with alternative electron acceptors. Permeable sands, such as the MAB sediments, are frequently and extensively flushed with seawater containing both oxygen and sulfate. Hence, the sedimentary community is likely to comprise both (facultatively) aerobic microbes and aerotolerant sulfate reducers. The benthic microbial community at our study site, as analyzed by fluorescence in situ hybridization, was dominated by planctomycetes and members of the *Cytophaga/Flavobacterium* cluster (Rusch et al., 2003). Cultured species of either group degrade a variety of organic compounds, in most cases aerobically. Potentially, the dissolution of carbonate particles in the sediment could liberate additional DIC without oxygen consumption. While data are lacking to evaluate the plausibility of carbonate dissolution and to estimate its significance as a source of DIC, the possibility cannot be ruled out.

The activity of aerobic and anaerobic bacteria living in the permeable MAB sand may be controlled by the dynamics of the advective pore water flows that may change between downward, upward, lateral flows, and stagnancy (Huettel et al., 1996). The effects of changes in the pore water flows on the metabolic processes in the sediment are reflected in the results of our *flow rate experiment* and the observation of SOC after different periods of pore water stagnancy. For example, in cores D1 and D2, the highest SOC were measured after long phases of stagnancy, whereas the measurements in D3 and D4 were preceded by less than 1 h of stagnancy after retrieval of the cores and resulted in very low SOC values (Table I). During stagnancy, reduced compounds form and accumulate, thus elevating the sedimentary oxygen demand during early phases of a subsequent flow period.

In situ, both interstitial flow rates and enzymatic activities decreased with sediment depth (Rusch et al., 2003; Reimers et al., 2004), whereas our experiments applied vertically homogeneous flow and measured depth-integrated turnover rates. Despite this limitation, they illustrate effects of interfacial and interstitial water flow on sandy seafloors. Between the constantly flushed top layer and the deep horizons without interstitial flow, a significant volume of permeable sediment experiences fluctuating flow and correspondingly variable biogeochemical conditions. Facilitating a wider spectrum of metabolic pathways, redox oscillation can enhance microbial activity and, thus, promote the degradation of organic matter (Aller, 1994; Sun et al.,

2002). Arguably, maximum benthic respiration rates are ultimately determined by the concentration (Figure 4) and quality of organic matter available, and by the metabolically active biomass. Within this frame, the actual rates appear to depend on pore water flow velocity. During early phases of the flow rate experiment, when transient state prevailed, SOC was significantly influenced by flow rate (Figure 2), whereas after >16 h, SOC was close to maximal and independent of flow rate, indicating that the supply of reactants to the benthic microbial community had reached saturation. The higher maximum rate in May as compared to July could be an effect of microbial abundances. In sandy shelf sediments, advective pore water flow generates transient state, in which the benthic mineralization potential is used less efficiently than in steady state. The same flow, however, greatly increases the mineralization potential by enhancing the supply of oxidants and organic substrates, which is likely to outweigh the loss of efficiency.

The *hydrolysis experiment* demonstrated that the passage of biopolymers through the MAB sand cores, as caused in situ by advective pore water flows at sediment ripples, leads to their glucoytic degradation. Cultured species of planctomycetes and the *Cytophaga/Flavobacterium* cluster are known to degrade biopolymers, and these groups were highly abundant in the microbial community inhabiting the sandy MAB sediments (Rusch et al., 2003). In shipboard incubations of these sediments without experimental exposure to flow, considerable potential rates of carbohydrate (up to $12 \text{ nmol cm}^{-3} \text{ h}^{-1}$) and peptide hydrolysis (up to $70 \text{ nmol cm}^{-3} \text{ h}^{-1}$) were measured (Rusch et al., 2003), while β -glucosidic activity in cores J4 and J8 (Figure 5) corresponded to 21 and $29 \text{ nmol cm}^{-3} \text{ h}^{-1}$, respectively.

Strong sediment mixing, as documented by the ripple formation at the study site, and advective pore water flow are likely to support the simultaneous presence of aerobic and anaerobic bacteria in the flushed layer. Under the ripple crests, pore water from anoxic sediment layers is pumped to the surface and may carry anaerobic bacteria from deeper layers to the surface (Silliman et al., 2001). Likewise, oxic bottom water intruding the bed may carry aerobic bacteria into the sediment, besides providing oxygen for aerobic growth. The length of the pathway the water takes through rippled sediment beds depends on the ripple height and ripple spacing (Shum, 1992) and varies between less than 1 cm to 1 m or more. Organic compounds that are carried into and out of the sediment, possibly multiple times (Bacon, 1994), are gradually decomposed while passing through the interstitial.

The bacterial community in the permeable MAB shelf sediments can efficiently degrade dissolved organic matter transported with advective pore water flows, such as fermentation products (e.g., acetate) upwelling from deeper layers, or polysaccharides (e.g., diatom exopolymers) from the overlying water. As another ecologically important consequence of the advective supply of degradable matter and electron acceptors, the consumption rate of

the bed can change dramatically on spatial scales of centimetres and within hours to minutes. The microbial community inhabiting such sediments is likely to be adapted to such rapid changes, as we observed prompt reactions in the column experiments. Likewise, the subsurface community may also be responsive to changes in water column composition, for example caused by upwelling events, current shifts, tides, storms, plankton blooms or waste disposal.

We conclude that the permeable sands, which are common deposits in the shelf areas, are effective biocatalytical filters that should not be viewed as relatively inactive just because of their low organic content. Our experiments showed that percolation of water loaded with degradable solutes through only 6–10 cm long columns of the MAB surface sediment resulted in significant degradation of these compounds. Turnover rates depended on the rate of interstitial flow and on the amount of organic substrate in solution. With an estimated $1000 \text{ L m}^{-2} \text{ d}^{-1}$ of bottom water being pumped through the upper sediment layer (Reimers et al., 2004), sandy beds may, thus, contribute significantly to the cycling of carbon and nutrients in shelf environments.

Acknowledgments

The authors gratefully acknowledge captains and crew of RV Cape Henlopen for their support during sampling. We appreciate the diving and general assistance of Charlotte Fuller, Rose Petrecca, and Susan Boehme from Rutgers University. This research was funded by the U.S. National Science Foundation (NSF) and the Max Planck Society (MPG), Germany.

References

- Aller R. C. (1994) Bioturbation and remineralization of sedimentary organic matter: Effects of redox oscillation. *Chem. Geol.* **114**, 331–345.
- Andersen F. Ø. and Helder W. (1987) Comparison of oxygen microgradients, oxygen flux rates and electron transport system activity in coastal marine sediments. *Mar. Ecol. Progr. Ser.* **37**, 259–264.
- Bacon M. P., Belostock R. A. and Bothner M. H. (1994) ^{210}Pb balance and implications for particle transport on the continental shelf, U.S. Middle Atlantic Bight. *Deep Sea Res. II* **41**, 511–535.
- Bélangier C., Desrosiers B. and Lee K. (1997) Microbial extracellular enzyme activity in marine sediments: Extreme pH to terminate reaction and sample storage. *Aquat. Microb. Ecol.* **13**, 187–196.
- Berg P., Røy H., Janssen F., Meyer V., Jørgensen B. B., Huettel M. and de Beer D. (2003) Oxygen uptake by aquatic sediments measured with a novel non-invasive eddy-correlation technique. *Mar. Ecol. Progr. Ser.* **261**, 75–83.
- Boetius A. and Lochte K. (1994) Regulation of microbial enzymatic degradation of organic matter in deep-sea sediments. *Mar. Ecol. Progr. Ser.* **104**, 299–307.

- Böttcher M. E., Hespeneheide B., Llobet-Brossa E., Beardsley C., Larsen O., Schramm A., Wieland A., Böttcher G., Berninger U. G. and Amann R. (2000) The biogeochemistry, stable isotope geochemistry, and microbial community structure of a temperate intertidal mudflat: An integrated study. *Continental Shelf Res.* **20**, 1749–1769.
- Dauwe B., Middelburg J. J. and Herman P. M. J. (2001) The effect of oxygen on the degradability of organic matter in subtidal and intertidal sediments of the North Sea area. *Mar. Ecol. Progr. Ser.* **215**, 13–22.
- Falter J. L. and Sansone F. J. (2000) Hydraulic control of pore water geochemistry within the oxic-suboxic zone of a permeable sediment. *Limnol. Oceanogr.* **45**, 550–557.
- Forster S., Huettel M. and Ziebis W. (1996) Impact of boundary layer flow velocity on oxygen utilization in coastal sediments. *Mar. Ecol. Progr. Ser.* **143**, 173–185.
- Hall P. O. J. and Aller R. C. (1992) Rapid, small-volume, flow injection analysis for ΣCO_2 and NH_4^+ in marine and freshwaters. *Limnol. Oceanogr.* **37**, 1113–1119.
- Holmer M. (1996) Composition and fate of dissolved organic carbon derived from phytoplankton detritus in coastal marine sediments. *Mar. Ecol. Progr. Ser.* **141**, 217–228.
- Huettel M. and Gust G. (1992) Impact of bioroughness on interfacial solute exchange in permeable sediments. *Mar. Ecol. Progr. Ser.* **89**, 253–267.
- Huettel M. and Rusch A. (2000) Transport and degradation of phytoplankton in permeable sediment. *Limnol. Oceanogr.* **45**, 534–549.
- Huettel M., Ziebis W., Forster S. and Luther III G. W. (1998) Advective transport affecting metal and nutrient distributions and interfacial fluxes in permeable sediments. *Geochim. Cosmochim. Acta* **62**, 613–631.
- Huettel M., Ziebis W. and Forster S. (1996) Flow-induced uptake of particulate matter in permeable sediments. *Limnol. Oceanogr.* **41**, 309–322.
- Kerkhof L. J., Voytek M. A., Sherrell R. M., Millie D. and Schofield O. (1999) Variability in bacterial community structure during upwelling in the coastal ocean. *Hydrobiologia* **401**, 139–148.
- Klimant I., Meyer V. and Kühl M. (1995) Fiber-optic oxygen microsensors, a new tool in aquatic biology. *Limnol. Oceanogr.* **40**, 1159–1165.
- Kristensen E. and Hansen K. (1995) Decay of plant detritus in organic-poor marine sediment: Production rates and stoichiometry of dissolved C and N compounds. *J. Mar. Res.* **53**, 675–702.
- Llobet-Brossa E., Rosselló-Mora R. and Amann R. (1998) Microbial community composition of Wadden Sea sediments as revealed by fluorescence *in situ* hybridization. *Appl. Environ. Microbiol.* **64**, 2691–2696.
- Newell R. C. (1970) *Biology of Intertidal Animals*. American Elsevier, New York.
- Pilditch C. A., Emerson C. W. and Grant J. (1998) Effect of scallop shells and sediment grain size on phytoplankton flux to the bed. *Continental Shelf Res.* **17**, 1869–1885.
- Precht E., Franke U., Polerecky L. and Huettel M. (2003) Oxygen dynamics in permeable sediments with wave-driven pore water exchange. *Limnol. Oceanogr.* **48**, 1674–1684.
- Reimers C. E., Stecher III H. A., Taghon G. L., Fuller C. M., Huettel M., Rusch A., Ryckelynck N. and Wild C. (2004) *In situ* measurements of advective solute transport in permeable shelf sands. *Continental Shelf Res.* **24**, 183–201.
- Revsbech N. P. (1989) An oxygen microsensor with a guard cathode. *Limnol. Oceanogr.* **34**, 474–478.
- Røy H., Huettel M. and Jørgensen B. B. (2002) The role of small-scale sediment topography for oxygen flux across the diffusive boundary layer. *Limnol. Oceanogr.* **47**, 837–847.
- Rusch A., Forster S. and Huettel M. (2001) Bacteria, diatoms and detritus in an intertidal sandflat subject to advective transport across the water-sediment interface. *Biogeochemistry* **55**, 1–27.

- Rusch A. and Huettel M. (2000) Advective particle transport into permeable sediments – evidence from experiments in an intertidal sandflat. *Limnol. Oceanogr.* **45**, 525–533.
- Rusch A., Huettel M. and Forster S. (2000) Particulate organic matter in permeable marine sands – dynamics in time and depth. *Estuarine, Coast. Shelf Sci.* **51**, 399–414.
- Rusch A., Huettel M., Reimers C. E., Taghon G. L. and Fuller C. M. (2003) Activity and distribution of bacterial populations in Middle Atlantic Bight shelf sands. *FEMS Microbiol. Ecol.* **44**, 89–100.
- Scala D. J. and Kerkhof L. J. (2000) Horizontal heterogeneity of denitrifying bacterial communities in marine sediments by terminal restriction fragment length polymorphism analysis. *Appl. Environ. Microbiol.* **66**, 1980–1986.
- Shum K. T. (1992) Wave-induced advective transport below a rippled water–sediment interface. *J. Geophys. Res. – Oceans* **97**, 789–808.
- Silliman S. E., Dunlap R., Fletcher M. and Schneegurt M. A. (2001) Bacterial transport in heterogeneous porous media: Observations from laboratory experiments. *Water Res. Res.* **37**, 2699–2707.
- Skopp J. M. (2000) Physical properties of primary particles. In *Handbook of Soil Science* (ed. M. E. Sumner), Chap. 1, pp. A3–A17. CRC Press, Boca Raton.
- Styles R. B. (1998) A continental shelf bottom boundary layer model: Development, calibration and applications to sediment transport in the Middle Atlantic Bight. PhD thesis, Rutgers University, New Brunswick NJ, 261 pp.
- Sun M.-Y., Aller R. C., Lee C. and Wakeham S. G. (2002) Effects of oxygen and redox oscillation on degradation of cell-associated lipids in surficial marine sediments. *Geochim. Cosmochim. Acta* **66**, 2003–2012.
- Thibodeaux L. J. and Boyle J. D. (1987) Bedform-generated convective transport in bottom sediment. *Nature* **325**, 341–343.
- Thomsen U. and Kristensen E. (1997) Dynamics of ΣCO_2 in a surficial sandy marine sediment: The role of chemoautotrophy. *Aquat. Microb. Ecol.* **12**, 165–176.
- Webb J. E. and Theodor J. (1968) Irrigation of submerged marine sands through wave action. *Nature* **220**, 682–685.
- Wilde S. B. and Plante C. J. (2002) Spatial heterogeneity of bacterial assemblages in marine sediments: The influence of deposit feeding by *Balanoglossus aurantiacus*. *Estuarine, Coast. Shelf Sci.* **55**, 97–107.
- Winkler L. W. (1888) The determination of dissolved oxygen in water. *Berichte der Deutschen Chemischen Gesellschaft* **21**, 2843–2857.
- Wollast R. (1991) The coastal organic carbon cycle: fluxes, sources, and sinks. In *Ocean Margin Processes in Global Change* (eds. R. F. C. Mantoura, J. M. Martin and R. Wollast). John Wiley & Sons, New York.
- Ziebis W., Huettel M. and Forster S. (1996) Impact of biogenic sediment topography on oxygen fluxes in permeable sediments. *Mar. Ecol. Progr. Ser.* **140**, 227–237.